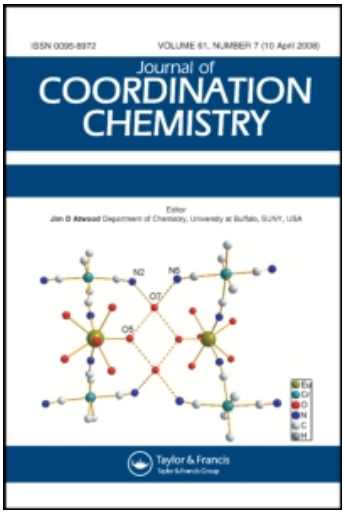

Journal of Coordination Chemistry
Publication details, including instructions for authors and subscription information:
http://www.informaworld.com/smpp/title~content=t713455674

The interactions of metal ions with nonsteroidal anti-inflammatory drugs (oxicams)

Nadia E. A. El-Gamel[a]
[a] Faculty of Science, Chemistry Department, Cairo University, 12613 Giza, Egypt

To cite this Article El-Gamel, Nadia E. A.(2009) 'The interactions of metal ions with nonsteroidal anti-inflammatory drugs (oxicams)', Journal of Coordination Chemistry, 62: 14, 2239 — 2260
To link to this Article: DOI: 10.1080/00958970902822630
URL: http://dx.doi.org/10.1080/00958970902822630

Journal of Coordination Chemistry
Vol. 62, No. 14, 20 July 2009, 2239–2260

Taylor & Francis
Taylor & Francis Group

The interactions of metal ions with nonsteroidal anti-inflammatory drugs (oxicams)

NADIA E. A. EL-GAMEL*

Faculty of Science, Chemistry Department, Cairo University, 12613 Giza, Egypt

(*Received 18 May 2008; in final form 18 November 2008*)

Much work has been focused on interactions of metal ions with nonsteroidal anti-inflammatory drugs (oxicams). Numerous attempts to synthesize several metal complexes have been published. This review highlights the synthesis and properties of the synthesized metal complexes. Different physico-chemical methods (IR, UV–Vis, measurement, thermal analysis, and NMR spectroscopy) as well as the bioactivity of the metal compounds are mentioned.

Keywords: Oxicams; Piroxicam; Tenoxicam; Meloxicam; Lornoxicam; Isoxicam; Crystal structures, Spectroscopy; Bioactivity

1. Introduction

Nonsteroidal anti-inflammatory drugs of the oxicam family have been pursued because of their potential applications and biological properties. Piroxicam [H_2pir, 4-hydroxy-2-methyl-*N*-(2-pyridyl)-2H-1, 2-benzothiazine-3-carboxamide-1, 1-dioxide], tenoxicam [H_2ten, 4-hydroxy-2-methyl-*N*-(2-pyridin-2-yl)-2H-thieno(2, 3-e)-1, 2-thiazine-3-carboxamide-1, 1-dioxide], meloxicam [H_2mel, 4-hydroxy-2-methyl-*N*-(5-methyl-2-thiazolyl)-2H-1, 2-benzothiazine-3-carboxamide-1, 1-dioxide], lornoxicam [H_2lorn, 8-chloro-4-hydroxy-2-methyl-*N*-(2-pyridyl)-2H-thieno(2, 3-e)-1, 2-thiazine-3-amide-1, 1-dioxide], and isoxicam [H_2iso, 4-hydroxy-2-methyl-*N*-(5-methyl-3-isoxazolyl)-2H-1, 2-benzothiazine-3-carboxamide-1, 1-dioxide] are oxicam drugs used in inflammatory and arthritic rheumatic diseases [1] and are the most studied species of the family because of their potential activity in biomedical chemistry and being strong chelators for metal ions. Scheme 1 represents the formulas of the oxicams mentioned in this review.

Many studies have centered on the different coordination modes of these drugs toward metal ions, i.e. H_2pir is a monodentate ligand through pyridyl N with Pt(II) [2], a bidentate ligand through its pyridyl N and amide O with Cu(II) and Cd(II) [3], and tridentate ligand via the enolic oxygen and amide nitrogen and pyridyl nitrogen with the organotin [4].

*Email: nadinealy@hotmail.com

Journal of Coordination Chemistry
ISSN 0095-8972 print/ISSN 1029-0389 online © 2009 Taylor & Francis
DOI: 10.1080/00958970902822630

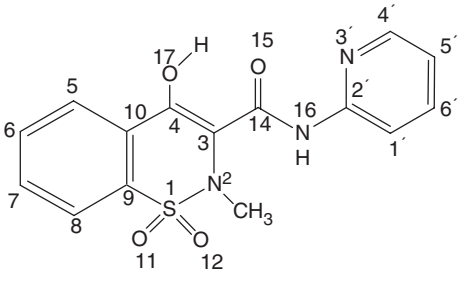

Piroxicam, H_2pir

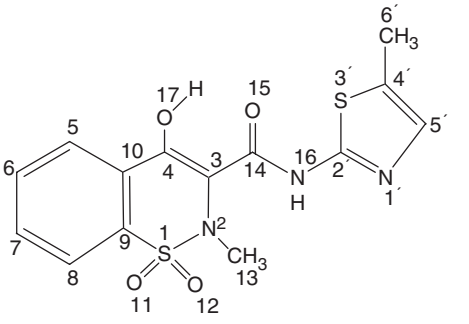

Meloxicam, H_2mel

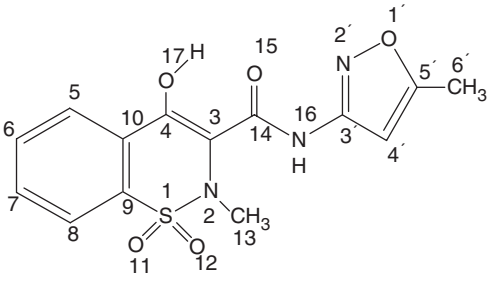

Isoxicam, H_2iso

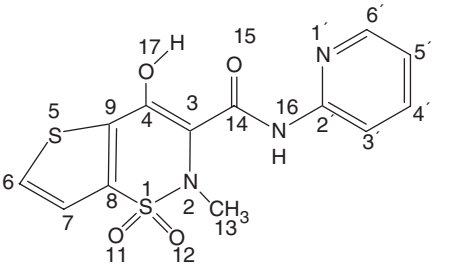

Tenoxicam, H_2ten

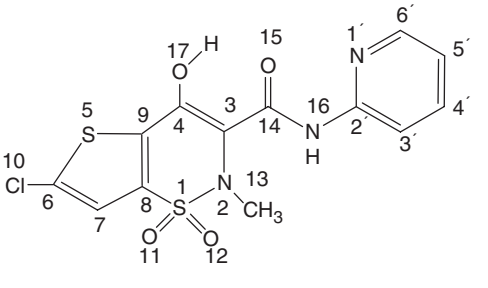

Iornoxicam, H_2lorn

Scheme 1. The formulas of oxicam molecules reported in the text.

Various analytical methods have been reported to investigate tenoxicam [5–11]; interactions with Fe(III), Co(II), Ni(II), Cu(II), and Mn(II) revealed that H_2ten is a monoanionic ligand through the enolate and amide oxygens [12]; on the other hand, coordination through the amide oxygen and pyridyl nitrogen have been shown for

$[Cu(Hten)_2(py)_2] \cdot EtOH$ and $Cd(Hten)_2(DMSO)_2$ [6, 13]. Differential pulse polarography and cyclic voltammetry studies with Cu(II), Pb(II), and Cd(II) complexes of H_2ten and H_2pir [14] show H_2ten with stronger chelating properties than H_2pir irrespective of their structural similarity. Furthermore, interactions of H_2ten with Fe(III), Sb(III), Bi(III), Cr(II), Cd(II), and Al(III) have been studied using potentiometric and fluorimetric techniques [15].

Interaction of tin(IV) with H_2ten, H_2pir, and H_2lor has been extensively studied due to their potential application as tin-based antitumor drugs [16].

In 2003, Defazio *et al*. presented a detailed investigation of meloxicam followed by preparation and structural characterization of Co(II), Ni(II), Zn(II), and Cd(II) complexes, where $Hmel^-$ anions chelated the metal center through the nitrogen from the thiazole ring and the amide oxygen [17]; in addition, the reactions of Cu(II) with H_2mel and H_2iso showed that coordination of Cu(II) by NSAIDs improved the pharmaceutical activity of the drugs themselves and reduced their undesired toxicity effects in human and veterinary medicine [18].

Spectroscopic and magnetic properties have been reported for Co(II), Ni(II), Cu(II), Zn(II), and Fe(III) with $Hiso^-$, where it acted as a monoanionic ligand coordinated to the metal through the enolate O atom and the carbonyl O atom of the amide group [19]. Direct electro-synthesis of Cu(II), Cd(II), and Zn(II) complexes of H_2pir and H_2iso have been reported [20].

To increase the activity of tenoxicam, complex formation of H_2ten with Cu(II) and Zn(II) were studied [21]. Considerable attention has been devoted to complex formations of α-, β-, γ-cyclodextrin with H_2pir, H_2ten, H_2mel, and H_2lor to improve aqueous solubility of the drugs as well as decrease their side effects [22].

Different types of binary and ternary metal complexes of H_2ten and H_2pir with some aminoacids have been reported to explore the different chelating modes for both drugs [23, 24]. In this review, studies of the preparation, structural characterization, and biological activity of oxicam complexes are summarized.

2. Crystal structures of oxicams and their metal compounds

2.1. *Free drugs*

Crystal structures of several free H_2pir [25], H_2ten [26], and H_2mel [27] molecules have been reported whereas H_2iso and H_2lor are rarely investigated and no crystal structures have been reported so far. H_2pir has been found to crystallize in neutral [25a, b] as well as zwitterionic form, where the enolic hydroxyl hydrogen has been transferred to pyridine nitrogen [25c, d] (scheme 2) while H_2ten has been crystallized in zwitterionic form [26] (scheme 2). H_2mel crystallized in four different protrotropic forms; the anion, the cation, the acidic enol, and the zwitterionic forms [27b] (scheme 2).

2.2. *Synthesis of metal complexes*

All oxicams are insoluble in water; therefore, all syntheses have been done in hot EtOH, hot MeOH, DMSO, or benzene. Some mixed ligand complexes have been prepared

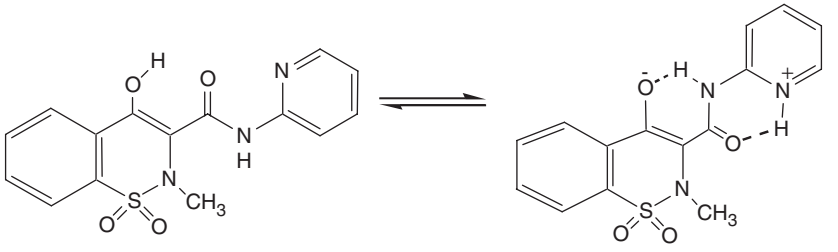

Piroxicam, H_2pir

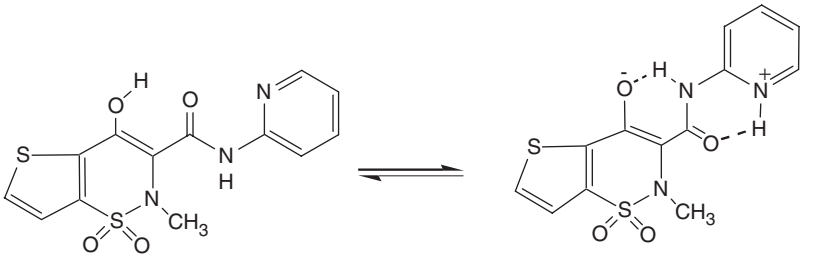

tenoxicam, H_2ten (EZE)

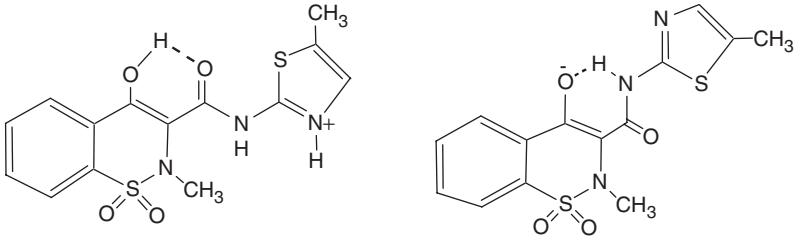

Cationic form of meloxicam anionic form of meloxicam

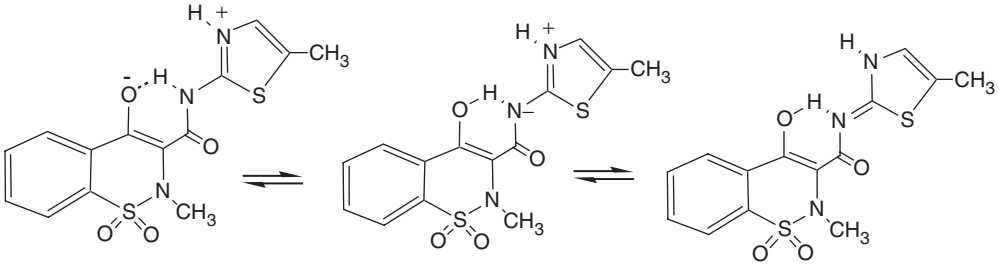

Zwitterionic form of meloxicam

Scheme 2. Zwitterionic forms of piroxicam, tenoxicam, and meloxicam.

and isolated. All structures of binary complexes are discussed below taking into consideration the numbering from original articles that have been used throughout the text.

2.3. *Cobalt complexes*

The complex Co(II)$(Hmel)_2(DMSO)_2$ [17] was prepared from hot MeOH solution of meloxicam and cobalt acetate; afterwards, the obtained crude solid was recrystallized from DMSO, while Co(II)$(Hten)_2(DMSO)_2$ was isolated from dissociation of ternary cobalt complex [Co(II)$(H_2ten)(ala)Cl(H_2O)]\cdot 2H_2O$ in DMSO [24]. In both complexes the ambidentate DMSO coordinated to the metal ion through oxygen; the $Hten^-$ chelated the metal center through the nitrogen from pyridine and through the amidic oxygens, where as $Hmel^-$ anions chelated the metal through nitrogen of thiazole and through the amidic oxygen. Both $Hten^-$ and $Hmel^-$ are deprotonated at O17 and adopted 17,1-ZZZ conformation. The coordination sphere is pseudo-octahedral in both complexes with metal ions located on the inversion centers (figure 1). The chelating anion is stabilized by a strong intramolecular hydrogen bond involving O17 and N16 in case of $Hmel^-$ and O3 and N2 in case of $Hten^-$ {O···N, 2.558(3), 2.61(1) Å; ∠O···H–N, 137.9(5) and 143.4(2)° for Co(II)$(Hmel)_2(DMSO)_2$ and Co(II)$(Hten)_2(DMSO)_2$, respectively}.

The first complex crystallized in triclinic system with space group *P-1* while the second crystallized in monoclinic system with space group P_21/n.

The torsion angles C7–C6–C5–O3 [−3.8(1)°], C5–C6–C7–N2 [−2.30(1)°], and C5–C6–C7–O4 [179.5(3)°] in $Hten^-$ indicated the planarity of the O3–C5–C6–C7(O4)–N2 system; furthermore, in $Hmel^-$ the thiazole system maintained the co-planarity upon metal chelation.

2.4. *Copper complexes*

The complex Cu$(Hpir)_2(DMF)_2$ was prepared by mixing a hot methanol solution of piroxicam and copper acetate, where the obtained solid is recrystallized from DMF [3]. Piroxicam chelated to Cu through its carbonyl oxygen O(15) of the amide group and the pyridyl nitrogen N1′ where the axial positions are occupied by two DMF molecules bonded through their carbonyl (scheme 1). The torsion angles C15–C2–C4–O5 [+1.3(2)°], C4–C2–C15–N4 [−5.4(2)°], and C4–C2–C15–O4 [174(1)°] indicated that the chelation of Cu ion to $Hpir^-$ has little effect on the planarity of O4–C15–C2–C4–O5 system.

Cu$(Hpir)_2(DMSO)_2$ was isolated by Tamasi *et al*. [28], where the coordination sphere is pseudo-octahedral and the metal coordinated by two $Hpir^-$ molecules in a ZZZ conformation through the amide oxygen and the pyridine nitrogen. This structure is isomorphic with previously reported complexes M$(Hmel)_2(DMSO)_2$ [17].

$[Cu(Hmel)_2(DMF)]\cdot 0.25H_2O$ was synthesized upon heating alcoholic solutions of H_2mel and copper acetate in a 1 : 2 ratio, then the solid recrystallized using DMF [18]. In this compound, $Hmel^-$ adopted ZZZ conformation and linked to Cu ion through the thiazole N1′ nitrogen and the amide O15 oxygen. The coordination sphere was square pyramidal, where Cu–O15 and Cu–N1′ bond lengths average 1.935(6) and 1.962(5) Å, respectively, inconsistent with standard square planar copper complexes from the literature [29].

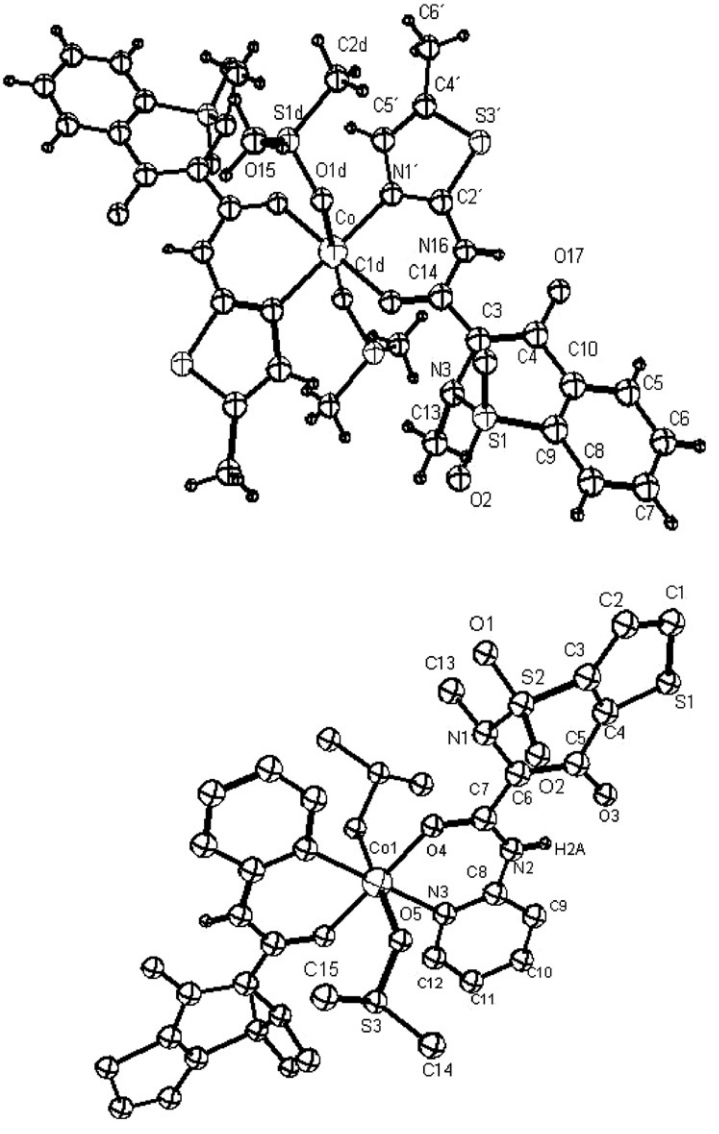

Figure 1. View of $[Co(II)(Hmel)_2(DMSO)_2]$ (on the top) (Ref. [17]) and $[Co(II)(Hten)_2(DMSO)_2]$ (on the bottom) (Ref. [24]). Most hydrogen atoms omitted for clarity.

The co-crystallized O_{1w} water formed a series of hydrogen bonds to methyl of DMF, C···O, 3.427(9) Å, ∠C–H···O, 127(1)° and to methyl of thiazole, O···O, 2.952(7) Å, and to O12, O···O, 2.798(7) Å (figure 2). The presence of π–π stacking involved DMF ligands; additionally, there are two Cu···S and two stacking interactions involving O=C–N(H)–thiazole moieties which stabilized the dimer.

$[Cu(Hiso)_2]\cdot 0.5DMF$ was prepared by heating mixed alcoholic solution of copper acetate to H_2iso in 1 : 2 ratio, then the solid residue recrystallized from DMF [18]. This structure was the first reported structure of an isoxicam metal compound.

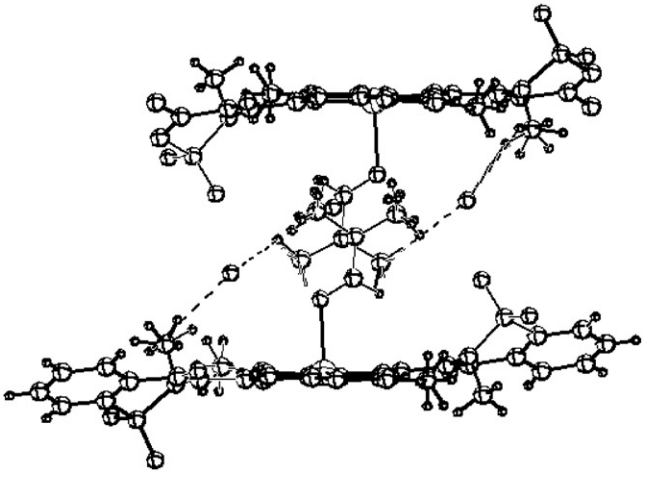

Figure 2. Prospective view of $[Cu(Hmel)_2(DMF)] \cdot 0.25H_2O$, representing the stacking π–π DMF···DMF interactions and the hydrogen bonds involved the co-crystallized water molecules and amide oxygen, and thio-dioxide oxygen atoms.

The coordination sphere is square planar. The two $Hiso^-$ anions behaved differently toward the copper, one anion adopted ZZZ conformation and chelated via amide oxygen O15 and isoxazole nitrogen N1′ while the second anion showed EZE conformation around the C3–C14, C14–N16, and N16–C2′ linkages and chelated through enolate oxygen O17 and amide oxygen O15 (figure 3). The conformation of the two ligand anions are from enolate oxygen from the EZE conformer *trans* to amide oxygen from the ZZZ one and the amide oxygen from EZE *trans* to nitrogen (isoxazole) from ZZZ. The *NO*– ZZZ ligand is stabilized by a strong intermolecular hydrogen bond N16–H···O7 [N···O, 2.511(5) Å, ∠N–H···O, 141(1)°], while the *OO*–EZE ligand is stabilized by two weaker intramolecular hydrogen bonds, N16–H···N2 [N···N, 2.716(5) Å; N–H···N, 108(1)°] and C3′–H···O15 [C···O, 2.772(6) Å; C–H···O, 108(1)°]. The *N*CN*C*O–ZZZ chelating system is planar as the torsion angle is $<1°$, while the *O*CCC*O*–EZE chelating system is more tilted, the torsion angles of O15–C14–C3–C4 and O17–C4–C3–C14 are $-6.6(4)$ and $6.8(4)°$, respectively. Due to the metal coordination to N1′, the double bond character of C2′–N1′ linkage is smaller for *NO*–ZZZ [C2′a–N1′a, 1.327(5) Å] than for *OO*–EZE [C2′–N1′, 1.314(4) Å] (figure 3). The DMF molecules are sandwiched between $Hiso^-$ molecules with interatomic contact lengths of 3.431(6) Å. There is a hydrogen bond from an isoxazole C3′ atom; C···O, 3.023(6) Å; ∠C–H···O, 136(1)° and other hydrogen bonds involving $Hiso^-$ anions and co-crystallized DMF. Further hydrogen bonds stabilize the crystal structure (figure 4). In the case of ZZZ–$Hiso^-$ anions, no significant hydrogen bonds are observed except a weak intramolecular hydrogen bond from C13 [C···O, 3.690(8) Å, ∠C–H···O, 162(1)°].

$Cu(Hiso)_2(THF)_2$ is obtained via procedure [28] similar to the procedure reported above [18]; the coordination sphere is pseudo-octahedral and the $Hiso^-$ anion adopted ZZZ conformation and coordinated to copper through O(amide) and N(isoxazole), with the enolate oxygen not participating in chelation due to involvement in an intramolecular N–H···O hydrogen bond.

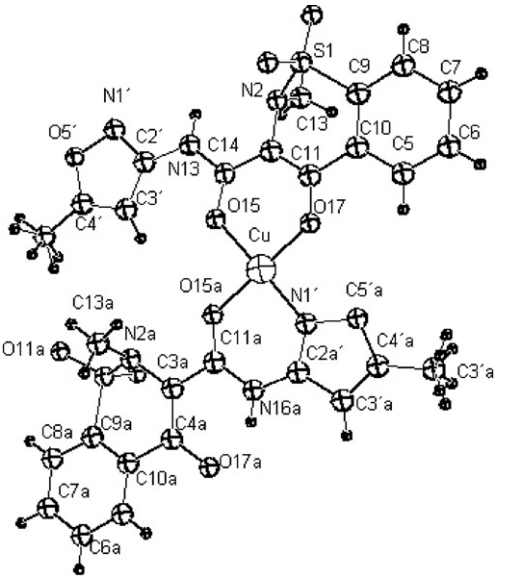

Figure 3. View of $[Cu(Hiso)_2] \cdot 0.5DMF$, Ref. [18].

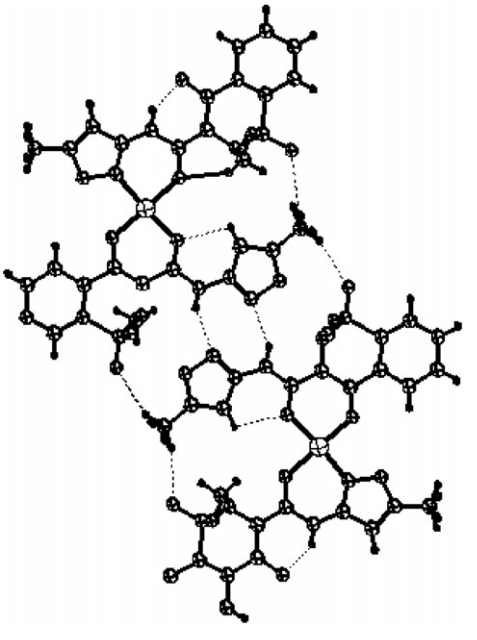

Figure 4. View of two $Cu(Hiso)_2$ molecules representing the hydrogen bonds by dashed lines, Ref. [18].

$[Cu(Hten)_2(py)_2] \cdot EtOH$ was synthesized by mixing hot pyridine solution of the ligand to Cu acetate where green precipitate was produced, which was recrystallized from pyridine–ethanol mixture [6]. Cu ion adopted pseudo-octahedral geometry with axial positions occupied by two pyridine molecules. The Cu–O1 and Cu–N1 bond lengths are 1.934(5) and 2.038(7) Å, respectively.

Oxygen O4 is involved in an intermolecular hydrogen bond [N2–H···O4, 2.575(6) Å], which is comparable with the zwitterionic form of the ligand (2.547 and 2.592 Å).

2.5. *Zinc complexes*

$Zn(II)(Hmel)_2(DMSO)_2$ was synthesized by reacting methanolic solution of the ligand and zinc acetate with recrystallization from DMSO [17]. This complex and $Co(II)(Hmel)_2(DMSO)_2$ are isostructural. The coordination spheres are pseudo-octahedral and zinc located on the inversion centers; the $Hmel^-$ chelated through N1′ nitrogen of the thiazole and through the O15 amidic oxygen at the equatorial positions (*trans* arrangement) and DMSO coordinated via oxygen.

The O17–C4 length in $Hmel^-$ ligand is 1.267(6), shorter than the value reported for H_2mel [1.336(2) Å] [27] and consistent with deprotonation at O17 and π-conjugation in the system (O17/N1′).

trans,*trans*-$[Zn(II)(Hten)_2(DMSO)_2]$ was synthesized by dissociation of $[Zn(II)(H_2ten)(ala)]Aco \cdot 3H_2O$ in DMSO [24]. As mentioned above, $Zn(II)(Hmel)_2(DMSO)_2$ is isostructural with $Co(II)(Hmel)_2(DMSO)_2$; *trans*,*trans*-$[Zn(II)(Hten)_2(DMSO)_2]$ is also isostructural with *trans*,*trans*-$[Co(II)(Hten)_2(DMSO)_2]$ [24]. The torsion angles C7–C6–C5–O3 [−3.7(2)°], C5–C6–C7–N2 [−2.50(2)°], C5–C6–C7–O4 [179.7(1)°] indicated the planarity of the C3–C5–C6–C7(O4)–N2 system as for *trans*,*trans*-$[Co(II)(Hten)_2(DMSO)_2]$.

2.6. *Cadmium complexes*

trans,*trans*-$[Cd(II)(Hmel)_2(DMSO)_2]$ was prepared by mixing methanolic solution of H_2mel and cadmium acetate and recrystallized from DMSO [17]. This structure is isostructural with the previous Co(II) and Zn(II) meloxicam complexes [17]. $Hmel^-$ is deprotonated at O17 and adopted 17,1′-ZZZ conformation; this anion is stabilized by strong intramolecular hydrogen bonds involving O17 and N16 atoms [O···N, 2.558(3) Å, ∠O···H–N, 137.9(5)°]. The thiazole system maintains co-planarity upon metal coordination. The O17–C4 bond length is 1.272(3) Å, shorter than the value found in $Hmel^-$ [1.336(2) Å] and similar to Co(II) and Zn(II) meloxicam complexes [17]; this is in agreement with deprotonation at O17 which allows significant π-conjugation in the system O17/N1′.

trans,*trans*-$[Cd(II)(Hpir)_2(DMF)_2]$ was prepared similar to the procedure mentioned for *trans*,*trans*-$[Cu(II)(Hpir)_2(DMF)_2]$ [3] and both compounds showed similar geometrical features. The coordination sphere is pseudo-octahedral and the $Hpir^-$ chelated via carbonyl oxygen O15 of the amido and pyridyl nitrogen N1. O17 is involved in a strong intramolecular hydrogen bond N–H···O with the N16···O17 distance of 2.581(6) Å.

$Cd(II)(Hten)_2(DMSO)_2$ was prepared by mixing 0.25 mmol of H_2ten to 0.125 mmol of cadmium acetate in hot methanol; the solid was recrystallized from DMSO [13]. This crystal structure is isostructural with Co(II) and Zn(II) tenoxicam complexes [24] with a pseudo-octahedral coordination sphere and the cadmium is located on the inversion center. $Hten^-$ is deprotonated at O17 and adopted 17,1′-ZZZ conformation, chelating through nitrogen from the pyridine (N1′) and through the amidic oxygen O15 at equatorial positions with a *trans* arrangement. $Hten^-$ is stabilized by strong

intermolecular hydrogen bonds which involved O17 and N16 atoms [O···N, 2.618(3) Å; ∠O···H–N, 143.5(2)°].

The torsion angles C14–C3–C4–O17 [−3.8(6)°], C4–C3–C14–N16 [−2.0(5)°], and C4–C3–C14–O15 [179.5(3)°] indicated the O17–C4–C3–C14(O15)–N16 segment is almost planar.

2.7. *Platinum complexes*

Cini [2a] prepared the first platinum complex of H_2pir with chemical formula $PtCl_2$(Hpir)(DMSO). This complex was synthesized from a mixture of $K_2[PtCl_4]$ and DMSO. The coordination sphere around Pt is almost planar. The largest deviation from canonical values is the angle Cl(1b)–Pt–Cl(2b) [175.0(1)°], where the metal deviates from the plane of the four donors by 0.027(2) Å; this deviation is toward H16. Each platinum is coordinated to two *trans* chlorides, to sulfur of DMSO and to N1′ from the pyridyl group (figure 5). The piroxicam ligand is neutral, protonated at O17 and has 4,16-EZE conformation as found in the solid-state structure of free H_2pir [25a]. Previously, ZZZ conformation was considered more stable by *ca* 3 Kcal mol^{-1} (*ca* 12.5 KJ mol^{-1}) than the EZE conformation using molecular mechanics analysis [30]. Hydrogen bond being the most effective explained the preference for ZZZ conformer. Intermolecular hydrogen bonds and van der Waals interaction can favor EZE in the solid state. Moreover, in this complex the presence of the Pt···HN interaction favored the EZE conformation.

In 1998 Di Leo *et al*. [2b] synthesized a platinum(II)–piroxicam complex by reaction of Zeise's salt K[$PtCl_3$](η^2-C_2H_4)]·H_2O with Hpir in ethanol at room temperature to produce *trans*-[$PtCl_2$(Hpir)(η^2-C_2H_4)]·0.5C_2H_5OH; crystals were obtained from benzene. Hpir coordinated through pyridyl N1′ and adopted EZE conformer. The coordination geometry is square planar, typical for platinum(II) complexes. Platinum is bound to two chlorides *trans* to each other, to N1′ from the pyridyl ring of Hpir and to an η^2-ethene (figure 6). Piroxicam in this complex does not undergo deprotonation at O17 and prefers the EZE conformation [2a]. This can be attributed to the low affinity of platinum for oxygen where it is difficult to enhance deprotonation of the OH and rearrange the conformation of Hpir into ZZZ. Chelation via O17 deprotonated and O15 in an EZE conformation is not probable due to the absence of stabilizing hydrogen bond O17···H–N16; this can be confirmed by formation of Pd(II)(Hpir)$_2Cl_2$ where H_2pir is remained neutral and does not chelate the metal center via O17 (protonated) and O15; unfortunately due to the lack of solubility of this compound in many solvents, no crystal structure can be afforded to completely characterize the molecular structure. Using IR, it was suggested that the palladium coordinated through N1′ of an EZE neutral H_2pir [2b].

trans-[PtCl(H_2ten)(η^2-C_2H_4)] was prepared by mixing $K_2[PtCl_4(\eta^2\text{-}C_2H_4)]\cdot H_2O$ with H_2ten in EtOH at room temperature with crystallization using benzene [13]. The coordination sphere of this compound is square planar [2a, b] with metal bonded to two chlorides (*trans* to each other), N1′ from pyridine and the ethylene.

H_2ten ligand adopted 17,1-EZE conformation with a strong intramolecular hydrogen bond between O17–H and the O15 [O–H···O, 2.63(1) Å; H···O, 2.00(1) Å; ∠O–H···O, 134(1)°]; some weak intramolecular hydrogen bonds are observed involving O15 and C3′ [O···H, 2.34(1) Å; O···C, 2.904(6) Å; ∠O–H···C, 119(1)°] and N2 and N16

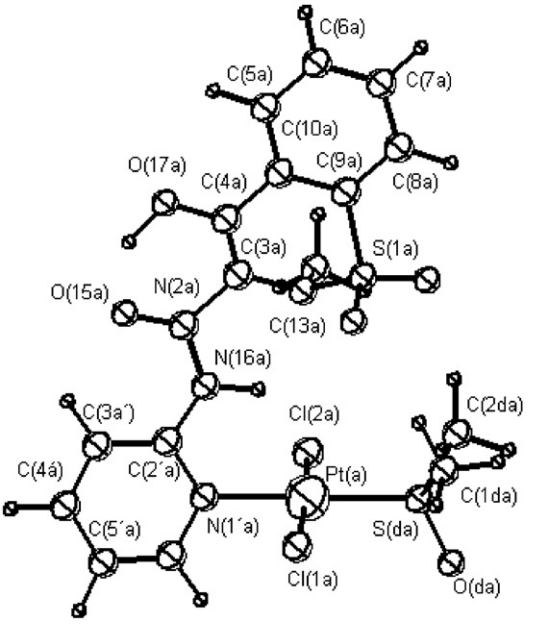

Figure 5. View of $PtCl_2$(Hpir)(DMSO), Ref. [2a].

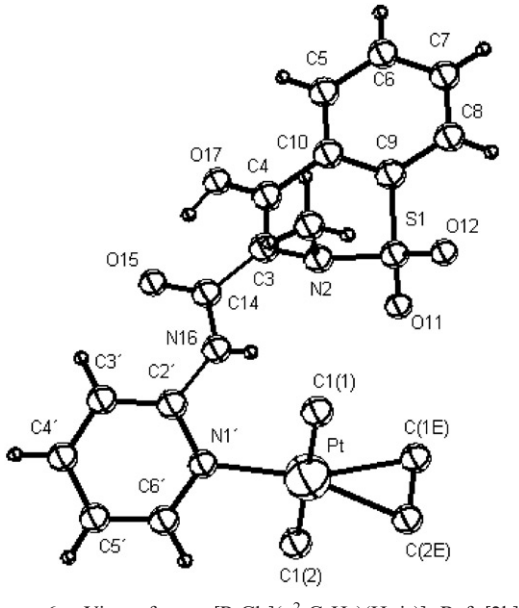

Figure 6. View of *trans*-[$PtCl_2$](η^2-C_2H_4)(Hpir)], Ref. [2b].

[N···H, 2.22(1) Å; N···N, 2.680(6) Å; ∠N–H···N, 113(1)°]. H_2ten behaved similarly to H_2pir in reactions with Zeise's salt where the ligand conformation preferred to be EZE.

The structure and preparation for *trans*-[$PtCl_2$(H_2mel)(η^2-(C_2H_4)] · 0.5C_6H_6 was similar to the previous procedure for *trans*-[$PtCl_2$(H_2ten)(η^2-(C_2H_4)] [13].

H_2mel ligand behaved similar to H_2ten and H_2pir regarding the reaction with Zeise's salt, where the sp^2-nitrogen is the only coordinated atom to platinum and the ligand conformation is EZE, stabilized by strong intramolecular hydrogen bond between O17–H group and O15 amidic atom [O···H, 1.91(1) Å, O···O, 2.62(2) Å; ∠O···H–O, 145.1(9)°]. The O17–C4–C3–C4(O15)–N16–C2′ system is almost planar.

2.8. *Organotin complexes*

$[SnBu_2(pir)]_n$ was synthesized from a methanolic solution of H_2pir with $SnBuCl_2$, with white powder obtained by slow evaporation of MeOH–MeCN solution [16c]. Figure 7 represents the crystal structure of the compound where two similar molecules in the asymmetric unit were observed. The stoichiometric ratio between Sn : pir is 1 : 1 and the ligand is a tridentate ligand coordinated to tin through enolic oxygen O1, amide N2, and pyridyl N1 nitrogens. The bond lengths of Sn–N pyridyl were very long, attributed to ring strain in the four-membered chelate ring and the low covalent character of the Sn–N pyridyl bond. H_2pir adopted EZZ configuration around C5–N2, N2–C6 and C6–C7, also found in the ethanolamine salt of H_2pir [31].

$SnBu_2$(ten) and $SnBu_2$(Hten)$_2$ were prepared from the reaction of H_2ten in benzene followed by addition of $SnBu_2O$ according to equations (1) and (2); single crystals were obtained from MeOH/MeCN mixture [16b].

$$SnBu_2O + H_2ten \rightarrow SnBu_2(ten) + H_2O \quad (1)$$

$$SnBu_2O + H_2ten \rightarrow SnBu_2(Hten)_2 + H_2O \quad (2)$$

As shown from the equations, organotin(IV) is coordinated by the singly charged anion $Hten^-$ in $SnBu_2$(Hten)$_2$ and by the doubly charged anion ten^{2-} in $SnBu_2$(ten). In $SnBu_2$(ten), ten^{2-} as doubly deprotonated ligand adopted EZZ configuration similar to that found for $[SnBu_2(pir)]_n$ [4]. Ten^{2-} coordinated as a tridentate ligand through enolic O (O4) and the amide N31 and pyridinyl N(1′), where two butyl C-atoms complete the five coordination sphere of organotin (figure 8). An intermolecular bond between tin and the neighboring ketonic O-atom have been observed with a distance Sn1···O31 of 2.650(3) Å. Further intermolecular hydrogen bonds of C–H···O type, inter- and intramolecular hydrogen bonds, C–H···π interaction stabilized the structure, similar to $SnBu_2$(pir) [16c].

The network of inter-and intramolecular hydrogen and non-hydrogen bonding can be attributed to the high electron density for the four O-atoms and for the pyridinyl and deprotonated amide-*N*-atoms in $SnBu_2$(ten). The same can be reported for $Hten^-$ where the high effective charge and electron density values for the enolate O and the amide O of $Hten^-$ showed strong electron donor properties; these interactions can produce aggregation and supramolecular assembly as mentioned for $SnBu_2$(pir) [16c].

$SnMe_2$(lorn) and $SnBu_2$(lorn) were the first reported structures of lornoxicam complexes by Galani *et al.* [16d], prepared through the interaction of SnR_2O (R is methyl or butyl) with lornoxicam (H_2lor) in benzene. Figure 9 represents the molecular structure for both compounds where the stoichiometric ratio between Sn : lorn is 1 : 1 and the ligand is tridentate, coordinated via the enolic oxygen O4 and the amide N31 and pyridyl N1′; two carbon atoms complete the five-fold coordination at the diorganotin(IV) fragment. In $SnBu_2$(lorn) there are two similar molecules in the

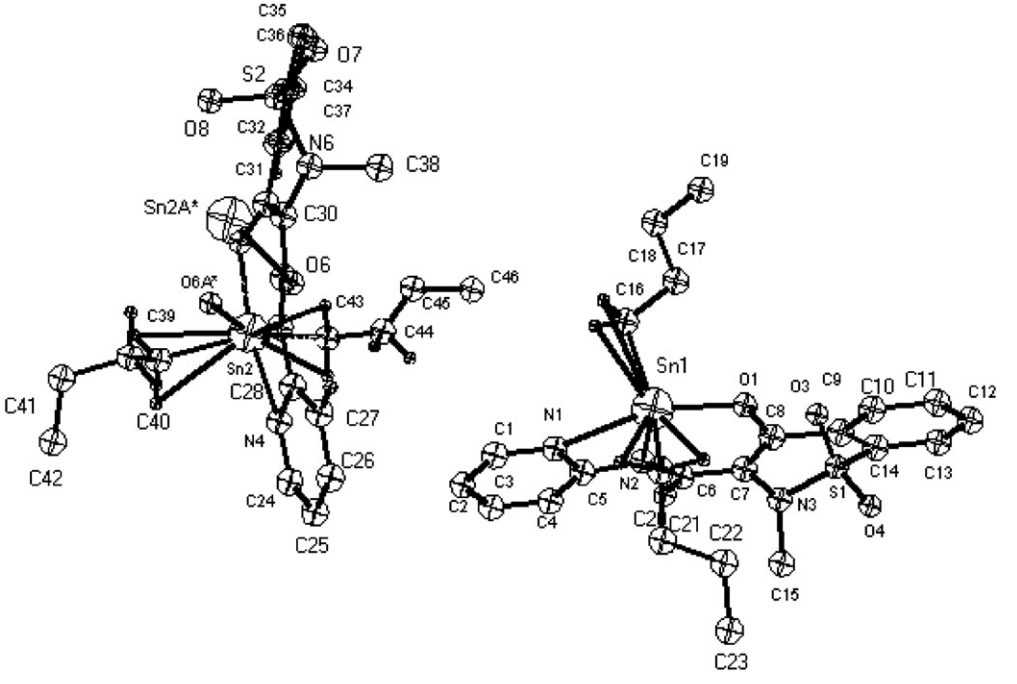

Figure 7. View of $[SnBu_2(pir)]_n$, Ref. [16c].

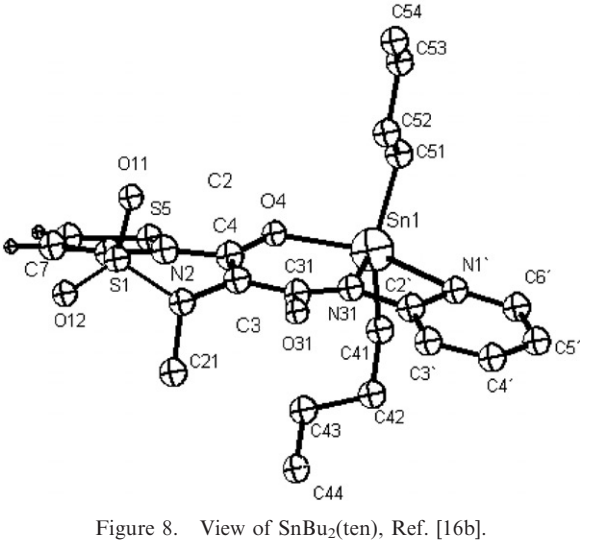

Figure 8. View of $SnBu_2(ten)$, Ref. [16b].

asymmetric unit. The di-anionic tridentate ligand adopted EZZ configuration around C2′–N31, N31–C31, and C31–C3 for both complexes. Although the EZZ configuration is less stable than the ZZZ one, deprotonation of amide nitrogen is important for EZZ configuration.

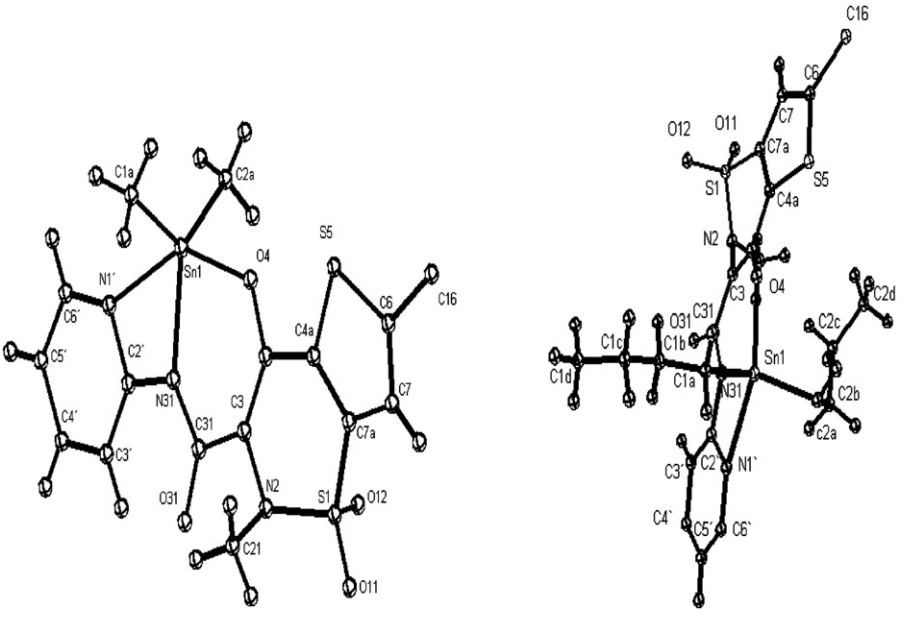

Figure 9. View of [$SnMe_2$(lorn)] (on the right) and [$SnBu_2$(lorn)] (on the left), Ref. [16d].

$SnMe_2$(lorn) crystallizes in a monoclinic crystal system whereas $SnBu_2$(lorn) crystallizes in a triclinic crystal system. The four oxygens, pyridyl, and imine nitrogens in the case of $SnMe_2$(Lorn) and $SnBu_2$(lorn) represent strong electron–donor properties and are involved in the extended network of inter- and intramolecular hydrogen and non-hydrogen bonding.

2.9. *Uranyl complexes*

cis-[$U(VI)O_2(Hten)_2(H_2O)] \cdot 2C_2H_5OH$ was synthesized by mixing $U(VI)O_2$ acetate to H_2ten in hot ethanol. Single crystals were obtained by recrystallization from ethanol [24]. The crystal structure of this compound is different from other complexes prepared from H_2ten ligand [13, 24] with two independent crystallographic molecules of Hten ligand in the asymmetric unit. The uranium is seven-coordinate, coordinated via enolate oxygen and carbonyl oxygen of amide group of two tenoxicam molecules and one water molecule. Mohamed [32] published without crystal structures uranyl complexes of H_2pir, where uranium was considered octahedral with coordination through pyridyl nitrogen and carbonyl oxygen of the amide. The $Hten^-$ adopted EZE conformation, stabilized by four hydrogen bonds (two from each side), two intramolecular hydrogen bonds between the amide nitrogen and their neighboring nitrogen from the other N1 and N5. [N2–H2A$\cdots$N1 = 2.680(1) Å; $\angle$ = 111.4(2)°; N5–H5A$\cdots$N4 = 2.681(3) Å; = 111.6(1)°]. Furthermore, the pyridyl nitrogen is involved in two intermolecular hydrogen bonds with the oxygen of the ethanol, but due to heavy disorder of the ethanol molecules over two positions these hydrogen bonds were not further discussed.

3. Thermal analysis

Only a few references are reported for the thermal behavior of free oxicams [26, 33]. Polymorphism is very common for oxicams with different melting point, solubilities, chemical reactivity, and stability. A series of binary and mixed ligand complexes of H_2pir and H_2ten in presence of amino acids like glycine or DL-phenylalanine or alanine with uranyl and transition metal ions were characterized by TG and DTA techniques [23a–e, 24]. In these systems, the complexes decomposed in two steps; dehydration is followed by decomposition of the anhydrous complexes to metal oxide or metal sulphide.

4. Infrared spectroscopy

All free oxicams show a broad band centered at ca. 3500–3400 cm^{-1} characteristic of O–H stretching [3, 16a, 16d, 17, 18]. The band at 3065 cm^{-1} is attributed to the N–H stretching vibration. The low frequency of these bands in free ligands may be explained by inter- and intramolecular hydrogen bonds involving the nitrogen and two oxygens of the secondary group [34]. ν(C=O) have a very strong band between 1630 and 1647 cm^{-1} with a shoulder in the range 1612–1619 cm^{-1} in all oxicams, while the band 1550–1596 cm^{-1} is assigned to C=N stretching of the pyridyl nitrogen [34, 35]. Two further bands in the range 1330–1351 cm^{-1} and 1040–1190 cm^{-1} are assigned to antisymmetric and symmetric stretching of the SO_2.

In $Cu(pir)_2(DMF)_2$ and $Cd(pir)_2(DMF)_2$, the band at 1630 cm^{-1} in free H_2pir shifts to 1610 cm^{-1}, representing chelation via amide oxygen [3]. The sharp band at 3340 cm^{-1} due to O–H disappears in the complexes due to deprotonation of the enolate O–H, as mentioned in the X-ray structure analysis [3].

Christofis *et al*. [36] characterized VO(II), Mn(II), Fe(III), MoO_2(II), and UO_2(II) complexes of H_2pir using different spectroscopic techniques. With H_2pir a bidentate to the metal through O amide and N pyridine, the ν(C=O) amide appeared at 1630 cm^{-1} and ν(C=N) pyridine at 1575 cm^{-1}. In all the complexes ν(C=O) amide is shifted to 1602–1625 cm^{-1} and ν(C=N) pyridine is shifted to 1558–1570 cm^{-1}, indicating coordination. The band due to O–H enolate group disappears in all the complexes, consistent with deprotonation of the enolate O–H. The N–H amide shifts from 3330 to 3180 cm^{-1} due to an intramolecular H-bond between the deprotonated enolic oxygen and the hydrogen of the amide N–H group.

The IR of *trans*-[$PtCl_2$(Hpir)(η^2-C_2H_4)] and *trans*-[$PdCl_2$(Hpir)$_2$] have bands at 3245 and 3293 cm^{-1}, respectively, for N–H stretching vibrations, red shifted at 91 and 97 cm^{-1} for *trans*-[$PtCl_2$(Hpir)(η^2-C_2H_4)] and *trans*-[$PdCl_2$(Hpir)$_2$], respectively, due to M···H–N interaction.

The IR spectra of H_2ten have a peak at 3386 cm^{-1} due to O–H stretch which disappeared for Mn(II), Fe(III), Co(II), Ni(II), and Cu(II) complexes [12], where H_2ten is the enolate anion; a broad absorption is observed in the 3380–3430 cm^{-1} region attributed to hydration water in the complexes. The secondary amide group at 1630 cm^{-1} in H_2ten lowers by 10–30 cm^{-1} in all the complexes indicating participation in complex formation [12]. Defazio and Cini [13] prepared Cd(II), Co(II), Zn(II), and Pt(II) compounds with H_2ten and Pt(II) and Fe(II) compounds with H_2mel with no

absorption attributed to N–H stretch observed in the complexes, consistent with the presence of intramolecular hydrogen bond between H–N(16) group and O16 atom for H_2ten in 17,1-ZZZ conformation. The absorption bands at 1635 and 1619 cm^{-1} for amidic C=O in H_2ten and H_2mel, respectively, shifts to 1615–1582 cm^{-1}. The N–H stretch has a maximum at 3244 and 3213 cm^{-1} for both Pt(II) complexes with a clear red shift of 75 cm^{-1} for *trans*-[$PtCl_2(H_2mel)(\eta^2$-$C_2H_4)$], due to Pt···H–N interactions similar to *trans*-[$PtCl_2(H_2pir)(\eta^2$-$C_2H_4)$] [2b] and *trans*-[$PtCl_2(H_2pir)$(DMSO)] [2a].

Demertzis *et al*. [16b] observed the low frequency of O–H and N–H bands in H_2ten indicative of inter- and intramolecular hydrogen bonds involving the N- and two O-atoms of the secondary amide group [35]. The neutral molecule exists in the zwitterionic form, adopting a planar conformation that is stabilized by two intramolecular H-bonds (N–H···O) [26a]. The ν(C=O) and ν(C=N) stretches of the secondary amide group –CO–NH– [35] at 1653, 1639, and 1596 cm^{-1} shift to 1600 and 1560 cm^{-1} for $SnBu_2$(ten) and 1638, 1599, and 1560 cm^{-1} for $SnBu_2(Hten)_2$. The $\nu_{asymmetric}$ and $\nu_{symmetric}$ (Sn–C_2) bands are observed at 507, 478 and 516, 479 cm^{-1} for $SnBu_2$(ten) and $SnBu_2(Hten)_2$, respectively, for a nonlinear Sn–C_2 moiety. $SnBu_2$(ten) showed bands at 237 and 217 cm^{-1} for ν(Sn–N_{pyr}) and ν(Sn–O) stretching modes while $SnBu_2(Hten)_2$ had bands at 216 and 206 cm^{-1} assigned to the ν(Sn–O) [37].

Fe(III), Co(II), Ni(II), Cu(II), and Zn(II) complexes with H_2iso were characterized spectroscopically [19]. In all the complexes, H_2iso is a monoanionic ligand coordinated through enolate oxygen and the carbonyl oxygen of the amide group. An absorption at 3290 cm^{-1} assigned to O–H group in H_2iso is absent for anhydrous Cu(iso)$_x$, attributed to coordination of Cu to anionic form of ligand through enolate. In all the remaining hydrated complexes a broad band is observed in the range 3000–3500 cm^{-1} due to hydrogen bonded water. A sharp band at 1633 cm^{-1} in free H_2iso assigned to the carbonyl stretching of the secondary amide group is shifted to 1620 cm^{-1} in all the complexes.

H_2lor ligand showed a broad absorption between 3500 and 3400 cm^{-1} characteristic of O–H stretch, while the N–H stretch is observed at 3067 cm^{-1}. Sharp bands at 1647, 1619, and 1596 cm^{-1} in H_2lor are assigned to the carbonyl C=O and the ν(C=N) of secondary amide group, shifted to 1619, 1591, and 1567 cm^{-1} for $SnMe_2$(lorn) and at 1600, 1599, 1578, and 1549 cm^{-1} for $SnBu_2$(lorn) [16d].

The $\nu_{asymmetric}$ and $\nu_{symmetric}$ (Sn–C_2) at 550, 473 and 551, 475 cm^{-1} for $SnMe_2$(lorn) and $SnBu_2$(lorn), respectively, indicate a nonlinear Sn–C_2. ν(Sn–N_{Pyr}) is observed at 265 and 268 cm^{-1} for $SnMe_2$(lorn) and $SnBu_2$(lorn), respectively; bands at 221 and 215 cm^{-1} for $SnMe_2$(lorn) and at 224 and 211 cm^{-1} for $SnBu_2$(lorn) are assigned to ν(Sn–O) [37].

5. UV–Vis spectroscopy studies

The changes in the UV part of oxicam spectra upon the addition of metal ions were studied by numerous authors [3, 12, 16d, 17–20, 23d, 61]. The UV spectrum of H_2pir in DMSO [36] showed a shoulder at 290 nm attributed to $n \rightarrow \pi^*$ transition of the C=O group of amide red shifted to 297–300 nm in the VO(II), Mn(II), UO_2(II), and MoO_2(II) and up to 310 nm in the Fe(III) complex, indicating complexation. The band at 355 nm in H_2pir attributed to $n \rightarrow \pi^*$ transition of the pyridyl nitrogen is red shifted

by 8–19 nm in all the complexes from donation of the lone pair of the pyridyl nitrogen to the metal ion (N → M) [23d]. For the $V(IV)O^{2+}$ complex, three low intensity bands at 785, 614, and 498 nm attributed to *d–d* transitions are observed. The spectrum of Fe(III) complex exhibits two bands attributed to *d–d* transitions, one very weak band at 605 nm ($\varepsilon = 18\,M^{-1}\,cm^{-1}$) assigned as a $^6A_{1g} \rightarrow {}^4T_{1g}$ transition and an intense one at $\lambda = 500$ nm ($\varepsilon = 108\,M^{-1}\,cm^{-1}$) assigned as a $^6A_{1g} \rightarrow {}^4T_{2g}(G)$ transition. Additionally, a shoulder at $\lambda = 418$ nm ($\varepsilon = 300\,M^{-1}\,cm^{-1}$) is attributed to a LMCT transition.

Cini *et al.* [3] recorded absorption spectra of Ni(II), Co(II), and Cu(II)–H_2pir complexes in DMSO and DMF; Ni(II) complex showed a weak band at 620 nm, while Cu(II) complexes in DMSO and DMF showed absorptions at 620 and 666 nm and a shoulder at 480 nm, respectively.

Mendez-Rojas *et al.* [20] reported UV spectra of Na(I), Cu(II), Cd(II), and Zn(II) metal ions with H_2pir and H_2isox. H_2pir showed absorption bands at 240 and 323 nm, while H_2isox at 318 nm. In all the complexes bathochromic shifts of 15–45 nm indicated coordination through the enolate.

Harrison *et al.* [19] described the UV spectra of H_2isox and Fe(III), Co(II), Ni(II), Cu(II), and Zn(II) complexes. In addition to *d–d* bands, bands at 10,500 and 16,667 cm^{-1} are assigned to the ν_1 and ν_2 transitions, with the ν_3 band obscured by the charge transfer edge. The reflectance spectrum of Fe(III) complex showed a shoulder at 20,000 cm^{-1} on the edge of the charge transfer band.

Defazio and Cini [17] reported the computed UV spectra of EZE–H_2mel in comparison with the Zn(II) complex. The computed spectrum showed a major band at 364 nm similar to the experimental absorption maximum at 343 nm in $CHCl_3$ due to charge transfer from thiazole to benzothiazine. The Zn(II) complex exhibited a peak at 333 nm due to the transition from thiazole to metal charge transfer transition.

The electronic spectrum of H_2lorn in DMF exhibited two broad bands at 398 and 273 nm [16d] assigned to $\pi \rightarrow \pi^*$ transitions. A broad band at *ca* 400 nm is assigned to a HOMO → LUMO transition, where the HOMO is π-centered on the sulfonamide and thiazine and the LUMO is mainly π-centered on the pyridyl ring. A broad band centered at 376 and 373 nm for $SnMe_2$(lorn) and $SnBu_2$(lorn), respectively, is assigned to a HOMO → LUMO transition, while broad bands at 292 and 295 nm for $SnMe_2$(lorn) and $SnBu_2$(lorn), respectively, are assigned to a combination of $\pi \rightarrow \pi^*$ and M → L transitions.

6. NMR spectroscopy

The ^{1}H- and ^{13}C-NMR spectra of oxicam ligands were recorded either in $CDCl_3$ or in DMSO-d_6 and assigned [3, 13, 16a, 16d, 17, 20, 23c, 23d, 24, 27b, 36, 38] and NMR has been used to analyze the drugs in their dosage forms [39]. Comparison of the ^{1}H- and ^{13}C-NMR of Hpir and $MoO_2(pir)_2$ in d_6-DMSO [36] show only significant changes in the pyridine ring (up to 0.49 ppm) upon complexation. A signal at 13.2 ppm is attributed to proton 16 that is twisted around the amide group and the resulting H-bond between the deprotonated enolic oxygen and the H of the N–H group.

The ^{13}C-NMR of Mo complex showed a downfield shift of the pyridyl carbons upon the complexation with C6′ and C2′ by 2.7 and 4.1 ppm, respectively; the other pyridyl carbons are shifted to higher field by 3 ppm. The amide carbonyl is shifted downfield.

Downfield shift by 4.8 ppm is observed for C4 due to H-bonding. Similar behavior is recorded for the UO_2(II) complex upon coordination through O_{amide} and $N_{Pyridyl}$.

^{1}H-NMR spectra have been recorded for Cu complexes with H_2pir [20], where all signals are shifted to higher fields relative to free ligand, attributed to coordination of the pyridine nitrogen N1′ of H_2pir. The signal of the proton attached to N17 is shifted to higher field due to formation of an intramolecular hydrogen bond.

^{1}H- and ^{13}C-NMR spectra were studied to characterize *trans*-$[PtCl_2(Hpir)(\eta^2\text{-}C_2H_4)]\cdot 0.5C_2H_5OH$ in $CDCl_3$ [2b], where the H(N) shifted to lower field by 1.98 ppm upon complexation. No coupling between ^{1}H(16) and ^{195}Pt nuclei was found. ^{13}C-NMR revealed a shift of the pyridyl carbons toward lower field by 0.8–4.0 ppm. The peaks of C2′ and C14 shift to higher field due to complexation. The signal of the ethane carbons is assigned at 78.7 ppm. ^{1}H-NMR of $Pt(Hpir)_2\cdot 3H_2O$ showed two peaks due to H–N(16) (δ 15.37, 15.87) and H_3C (δ 2.60, 2.90), respectively.

The characterization of H_2pir with β-cyclodextrin in solution has been done by ^{13}C-NMR [40] where piroxicam is in the zwitterionic monohydrated form.

Complexation of Zn(II) with H_2mel was studied by ^{1}H-NMR in $CDCl_3$ [17] with the H(N) amide downfield from 10.20 ppm for H_2mel to 9.66 ppm in the complex upon coordination through O15 and N1′. The signal of the thiazole C(5′)H proton at 7.43 ppm is downfield by 0.15 ppm upon chelation to thiazole.

^{1}H-NMR in DMSO-d_6 of *trans*,*trans*-[Cd(II)$(Hten)_2$] [13] show signal is shifted to higher field upon complex formation and deprotonation of O17; H(5′) and H(7) are shifted to 0.29 and 0.12 ppm, respectively. Chemical shifts for *trans*,*trans*-$[PtCl_2(\eta^2\text{-}C_2H_4)(H_2ten)]$ in $CDCl_3$ are shifted to lower field upon coordination to platinum through N1′. Similarly, for *trans*,*trans*-$[PtCl_2(H_2mel)(\eta^2\text{-}C_2H_4)]$ in $CDCl_3$ the signals are shifted to lower field with amidic H(16) by 1.26 ppm; this shift is smaller than in *trans*,*trans*-$[PtCl_2(H_2ten)(\eta^2\text{-}C_2H_4)]$ due to the larger H(16)$\cdots$Pt distance [13]. The signal for enolic H(17) is upshifted by 0.35 while in *trans*,*trans*-$[PtCl_2(H_2ten)(\eta^2\text{-}C_2H_4)]$ it is upshifted by 0.60 ppm.

Demertzis *et al.* [16b] reported ^{1}H- and ^{13}C-NMR spectra for H_2ten, $SnBu_2$(ten), and $SnBu_2(Hten)_2$ in $CDCl_3$. For $SnBu_2$(ten) the ortho proton of H(C6′) and C(6′) are deshielded by 8.51 and 141.9 ppm, respectively, attributed to the electrophilicity of tin. Upfield shift is observed for H–C4′ and C4′, para to the Sn due to π-back donation from the Sn into the aromatic ring [40]. The signals attributed to the NH and OH groups disappear upon interaction with the metal, indicating deprotonation and possible coordination to Sn. A tridentate coordination through the enolic O-atom and the amide and the pyridinyl N-atoms has recently been reported, similar to $[SnBu_2(pir)]_n$, where the ligand exists in doubly protonated form; ^{13}C-NMR showed disappearance of C4 signal while the C3 signal showed a downfield shift of 5.2 ppm. A similar behavior was observed for C6 (6.2 ppm). The bond between N1′ and Sn atom leads to downfield shift of C6′ by 3.4 ppm, while C4′ shifted to higher field by 5.0 ppm.

^{1}H- and ^{13}C-NMR spectra for H_2lor, $SnMe_2$(lorn) and $SnBu_2$(lorn) in $CDCl_3$ [16d] show disappearance of the downfield OH and NH signals due to loss of both hydrogens with metal complexation. OH signal is downfield at $\delta = 14.02$ ppm for H_2lorn, indicating hydrogen-bonding. In both complexes deshielding of H6′, H3′, and the corresponding carbon atoms C(6′), C(3′) is observed due to electrophilicity of tin. A σ-charge donation from N(1′)-donor to the tin center removed electron density from the ligand and produces this deshielding. The upfield shift observed for H4′ and H5′ and the corresponding carbons C(4′) and C(5′) *meta* and *para* to the tin center arise from π-back donation from

tin to the aromatic ring [16a–c]. The imino and hydroxyl signals disappeared upon complexation related to deprotonation and coordination to tin.

7. Bioactivity of oxicam–metal compounds

$Fe(Hpir)_3$, $VO(Hpir)_2(H_2O)$, and $MoO_2(Hpir)_2$ were tested in HL-60 leukemia cell line, regarding cytotoxicity, necotric effects with induction of apoptosis studied. Among the complexes, only $VO(Hpir)_2(H_2O)$ does not provoke a lot of necrotic cells and induces apoptosis after 24-h incubation, while piroxicam induced apoptosis after 57-h incubation [36].

The interaction of β-cyclodextrin with H_2pir and H_2ten reduced side effects of these drugs in the gastrointestinal tract and increased their clinical efficiency [22a]. Piroxicam-β-cyclodextrin was tested in treatment of patients with chronic acute nonspecific back pain and was effective to reduce the disease as well as the risk of direct-contact gastric irritation [41] and showed effective relief of acute pain and chronic diseases such as osteoarthritis [42]. The complexation of H_2ten with γ-, HPγ-, β-, HPβ- and Mβ-cyclodextrin in aqueous solution [22c, 22d] improved the percutaneous penetration of the drug through abdominal rat skin by increasing the solubility of the drug.

The anti-inflammatory activity and gastric lesions induced by zinc–tenoxicam complex were studied [43]; the severity of gastric lesions induced by oral treatment for 7 days using the complex was reduced compared to tenoxicam.

The binding of Cu(II)-piroxicam and Cu(II)-meloxicam with DNA backbone shows better anticancer properties [44], confirmed by Cini *et al*. [18] by testing the cytotoxic activity of Cu-oxicam complexes against tumor cell lines *in vitro* as well as anticancer activity.

Meloxicam reported for treatment of respiratory diseases in pigs [45] showed several applications in treatment of patients with colon cancer [46]. In addition to that, the β-CD complex of meloxicam showed ulcerogenic activity and reduced ulcer formation [22d].

As reported before, the interaction of tin(IV) with NSAIDs are heavily studied according to their potential application as antitumor drugs [16].

8. Conclusion

In this review, reports concerning the coordination chemistry of oxicams in particular, H_2pir, H_2ten, H_2mel, H_2iso, H_2lor drugs have been discussed. A range of metal complexes have been prepared with these drugs. We covered all reports concerning the synthesis of metal complexes and their investigation using different physiochemical tools like FTIR, UV–Vis, NMR, and thermal studies. The structures of the metal complexes are provided, to facilitate comparison, and we present table 1 to show the variety of coordination arrangements of the prepared complexes. The O17–C4–C3(O15)–N16–C2′ system maintained co-planarity upon metal chelation. In the case of transition metal complexes, all oxicam drugs adopted the ZZZ conformer, which is the most stable conformation according to molecular mechanics analysis. In the case

Table 1. Selected data of oxicam-metal complexes.

Formula of the complex [reference]	Atoms involved in the metal chelation	Coordination number of the central atom
$[Co(II)(Hmel)_2(DMSO)_2]$ [17]	O(P), N(P), O(DMSO)	6
$[Co(II)(Hten)_2(DMSO)_2]$ [24]	O(P), N(P), O(DMSO)	6
$[Cu(pir)_2(DMF)_2]$ [3]	O(P), N(P), O(DMF)	6
$[Cu(Hmel)_2(DMF)]\cdot 0.25H_2O$ [18]	O(P), N(P), O(DMF)	5
$[Cu(Hiso)_2]\cdot 0.5DMF$ [18]	O(P), N(P)	4
$[Cu(ten)_2(py)_2]$ EtOH [6]	O(P), O(C), N(P)	6
$[Zn(Hmel)_2(DMSO)_2]$ [17]	O(P), N(P), O(DMSO)	6
$[Zn(Hten)_2(DMSO)_2]$ [24]	O(P), N(P), O(DMSO)	6
$[Cd(Hmel)_2(DMSO)_2]$ [17]	O(P), N(P), O(DMSO)	6
$Cd(II)(pir)_2(DMF)_2]$ [3]	O(P), N(P), O(DMSO)	6
$[Cd(II)(Hten)_2(DMSO)_2]$ [13]	O(P), N(P), O(DMSO)	6
$[PtCl_2(Hpir)(DMSO)]$ [2a]	N(P), S(DMSO), Cl	4
$[PtCl_2](\eta^2\text{-}C_2H_4)(Hpir)]$ [2b]	N(P), Cl, C(E)	4
$[PtCl(\eta^2\text{-}C_2H_4)(H_2ten)]$ [13]	N(P), Cl, C(E)	4
$[PtCl_2(H_2mel)\eta^2\text{-}(C_2H_4)]\cdot 0.5C_6H_6$ [13]	N(P), Cl, C(E)	4
$[SnBu_2(pir)]_n$ [16c]	O(OH), O(P), N(P), C(Bu)	5
$[SnBu_2(ten)]$ [16b]	O(OH), O(P), N(P), C(Bu)	5
$[SnMe_2(lorn)]$ [16d]	O(OH), O(P), N(P), C(Me)	5
$[SnBu_2(lorn)]$ [16d]	O(OH), O(P), N(P), C(Bu)	5
$[U(VI)O_2(Hten)_2(H_2O)]\cdot 2C_2H_5OH$ [24]	O(OH), O(P), O(OH)	7

Notes: O(P), ring amide oxygen; O(C), ring carbonyl oxygen; O(OH), enolic oxygen; N(P), ring pyridyl nitrogen; C(E), ethylene carbon; C(Bu), butyl carbon; C(Me), methyl carbon.

of $[Cu(Hiso)_2]\cdot 0.5DMF$, the two $Hiso^-$ anions behaved differently with one anion showing ZZZ conformation while the other showed EZE conformation.

For Pt(II) complexes, EZE conformation is preferred due to the presence of Pt···HN interaction and according to the low affinity of Pt(II), where it is difficult to enhance deprotonation of the OH function and rearrange the conformation from EZE to ZZZ conformation. In organotin complexes, the favored conformer is EZZ due to deprotonation of amide nitrogen.

The formation and use of metal-oxicam complexes may extend the applications in bio-inorganic chemistry. The potential of these complexes has been exploited in the synthesis of interesting and important biologically-active compounds. We expect to see new and interesting chemistry of oxicam complexes in the near future.

References

[1] P. Emery, S.X. Kong, E.W. Ehrich, D.J. Watson, T.E. Towheed. *Clin. Therapeut.*, **24**, 1225 (2002).
[2] (a) R. Cini. *J. Chem. Soc., Dalton Trans.*, 111 (1996); (b) D. Di Leo, F. Berrettini, R. Cini. *J. Chem. Soc., Dalton Trans.*, 1993 (1998).
[3] R. Cini, G. Giorgi, A. Cinquantini, C. Rossi, M. Sabat. *Inorg. Chem.*, **29**, 5197 (1990).
[4] S.K. Hadjikakou, M.A. Demertzis, J.R. Miller, D. Kovala-Demertzi. *J. Chem. Soc., Dalton Trans.*, 663 (1999).
[5] E. Bernhard, F. Zimmermann. *Arzneim.-Forsch.*, **34**, 647 (1984).
[6] M.R. Moya-Hernández, A. Mederos, S. Domínguez, A. Orlandini, C.A. Ghilardi, F. Cecconi, E. González-Vergara, A. Rojas-Hernández. *J. Inorg. Biochem.*, **95**, 131 (2003).
[7] O. Atay, F. Dincol. *Anal. Lett.*, **30**, 1675 (1997).
[8] A.F.M. ElWalily, S.M. Blaih, M.H. Barary, M.A. ElSayed, H.H. Abdine, A.M. ElKersh. *J. Pharm. Biomed. Anal.*, **15**, 1923 (1997).

[9] Z. Atkopar, M. Tuncel. *Anal. Lett*., **29**, 2383 (1996).
[10] M.S. Garcia, C. Sanchez-Pedreno, M.I. Albero, M.J. Gimenez. *J. Pharm. Biomed. Anal*., **21**, 731 (1999).
[11] D.W. Blake, A.R. Bjorksten, F.C. Libreri. *Anaesth. Intensive Care*, **25**, 142 (1997).
[12] A. Bury, A.E. Underhill, D.R. Kemp, N.J. O'Shea, J.P. Smith, P.S. Gomm. *Inorg. Chim. Acta*, **138**, 85 (1987).
[13] S. Defazio, R. Cini. *Polyhedron*, **22**, 1355 (2003).
[14] N. Abo El-Maali, J.C. Vire, G.J. Patriarche, M.A. Ghandour. *Anal. Lett*., **2**, 3025 (1989).
[15] H.A. Mohamed, H.M.A. Wadood, O.A. Farghaly. *J. Pharm. Biomed. Anal*., **28**, 819 (2002).
[16] (a) D. Kovala-Demertzi. *J. Organomet. Chem*., **691**, 1767 (2006); (b) M.A. Demertzis, S.K. Hadjikakou, D. Kovala-Demertzi, A. Koutsodimou, M. Kubicki. *Helv. Chim. Acta*, **83**, 2787 (2000); (c) S.K. Hadjikakou, M.A. Demertzis, J.R. Miller, D. Kovala-Demertzi. *J. Chem. Soc., Dalton Trans*., 663 (1999); (d) A. Galani, M.A. Demertzis, M. Kubicki, D. Kovala-Demertzi. *Eur. J. Inorg. Chem*., 1761 (2003).
[17] S. Defazio, R. Cini. *J. Chem. Soc., Dalton Trans*., 1888 (2002).
[18] (a) R. Cini, G. Tamasi, S. Defazio, M.B. Hursthouse. *J. Inorg. Biochem*., **101**, 1140 (2007); (b) R. Cini. *Comments Inorg. Chem*., **22**, 151 (2000).
[19] D.O. Harrison, R. Thomas, A.E. Underhill, J.K. Fletcher, P.S. Gomm, F. Hallway. *Polyhedron*, **4**, 681 (1985).
[20] M.A. Mendez-Rojas, F. Cordova-Lozano, G. Gojon-Zorrilla, E. Gonzalez-Vergara, M.A. Quiroz. *Polyhedron*, **18**, 2651 (1999).
[21] for Zn(II) (a) J.W.L. Nascimento, L.H. Santos, M.S. Nothenberg, M.M. Coelho, S. Oga, C.A. Tagliati. *Pharmacology*, **68**, 64(2003). (b) J.W.L. Nascimento, C.A. Tagliati, M.S. Nothenberg, S. Oga, L.H. Santos, Braz. Pedido Pl (2001), BPXXDX BR 2099003666 A 20010522, Portuguese Patent. For Cu(II), (a) J.R. Sorenson. *J. Med. Chem*., **19**, 135 (1976). (b) J.R. Sorenson. *Prog. Med. Chem*., **26**, 437 (1989).
[22] For H_2pir: (a) Y. Zhou, G. Zhang, Z. Wang, H. Wang, C. Dong, S. Shuang. *J. Inclusion Phenom. Macrocyclic Chem*., **56**, 215 (2006). (b) R.C. Doijad, M.M. Kanakal, F.V. Manvi. *Indian Pharmacist*, **6**, 94 (2007). (c) M. Jug, M. Becirevic-Lacan, A. Kwokal, B. Cetina-Cizmek. *Acta Pharmaceutics*, **55**, 223 (2005). (d) S. Charumanee, P. Weiss-Greiler, P. Wolschann, H. Viernstein, A. Titwan, J. Sirithunyalug, S. Okonogi. *Sci. Pharm*., **73**, 147 (2005). (e) A. Capocchi. PIXXD2 WO 2003105906 A1 20031224 (2003). (f) *J. Maslarova. Farmatsiya*, **49**, 18 (2002). (g) A. Bertoluzza, M. Rossi, P. Taddei, E. Redenti, M. Zanol, P. Ventura. *J. Mol. Struct*., 480 (1999). For H_2ten: (a) R. Banerjee, H. Chakraborty, M. Sarkar. *Biopolymers*, **75**, 355 (2004). (b) Z. Aigner, A. Kezsmarki, M. Kata, C. Novak, I. Eroes. *J. Inclusion Phenom. Macrocyclic Chem*., **42**, 227 (2002). (c) E. Larrucea, A. Arellano, S. Santoyo, P. Ygartua. *Drug Dev. Ind. Pharm*., **28**, 245 (2002). (d) E. Larrucea, A. Arellano, S. Santoyo, P. Ygartua. *Drug Dev. Ind. Pharm*., **27**, 251 (2001). (e) J-H. Kim, H-K. Choi. *Yakche Hakhoechi*, **30**, 33 (2000). (f) L.J. Penkler, L.A. Glintenkamp, M.D. Bodley, M.C. Van Oudtshoom, C. Stubbs. PIXXD2 WO 9532737 A1 19951207 (1995). (g) T. Loftsson, B.J. Olafsdottir, H. Fridriksodottir, S. Jonsdottir. *Eur. J. Pharm. Sci*., 1, 95 (1993). (h) T. Loftsson, H. Fridriksodottir, S. Jonsdottir, O. Gudmundsson. *Acta Pharmaceutica Nordica*, **3**, 215 (1991). For H_2mel: (a) K.P.R. Chowdary, P. Raviprakash. *Int. J. Chem. Sci*., **4**, 845 (2006). (b) A.A. Abdoh, M.I. El-Barghouthi, M.B. Zughul, J.E. Davies, A.A. Badwan. *Pharmazie*, **62**, 55 (2007). (c) B.N. Nalluri, K.P.R. Chowdary, K.V.R. Murthy, V. Satyanarayana, A.R. Hayman, G. Becket. J. *Inclusion Phenom. Macrocyclic Chem*., **53**, 103 (2005). (d) S. Baboota, S.P. Agarwal. *Indian Pharmacist*, 4, 62 (2005). (e) S. Baboota, S.P. Agarwal. I*ndian J. Inclusion Phenom. Macrocyclic Chem*., 5**1**, 219 (2005). (f) Y. Sun, J. Shi, H. Zhong, Z. He, Z. Wang, H. Li. S*henyang Yaoke Duebao*, **21**, 81 (2004). (g) N.B. Naidu, K.P.R. Chowdry, K.V.R. Murthy, V. Satyanarayana, A.R. Hayman, G. Becket. J. *Pharm. Biomed. Anal*., **35**, 75 (2004). (h) S. Baboota, S.P. Ag*arwal. Pharmazie*, **58**, 73 (2003). (i) K. Gowthamarajan, T. Kulkarni, T. Girirai, G. Venkateswaran, M.K. Samanta, B. Suresh. I*nd. J. Pharm. Sci*., 6**4**, 525 (2002). (j) S. Baboota, S.P. Agarwal. *Ind. J. Pharm. Sci*., 6**4**, 408 (2002). (k) S.L. Sacurai, N. Augusto Filho. Portuguese Patent. BPXXDX BR 2099003221 A 20010306 (2001). For H_2lor: (a) H. Wang, Y. Wang, J. Ding. Y. Dou, H. Ma. Chinese Patent. CNXXEV CN 101015555 A 20070815 (2007). (b) Y. Gao, J.-J. Zhang, W.-M. Fan, B.-J. Ren. *Zhongguo Xiandai Yingyong Yaoxue*, **23**, 207 (2006). (c) Y.-N. Wang, H.-Q. Wang. *Jiefangjun Yaoxue Xuebao*, **22**, 146 (2006). (d) J.L. Penkler, D.V. Whittaker. PIXXD2 WO 9641646 A2 19961227 (1996).
[23] (a) M.A. Zayed, F.A. Nour El-Dien, G.G. Mohamed, N.E.A. El-Gamel. *Spectrochim. Acta*, **64A**, 216 (2006); (b) M.A. Zayed, F.A. Nour El-Dien, G.G. Mohamed, N.E.A. El-Gamel. *Spectrochim. Acta*, **60A**, 2843 (2004); (c) G.G. Mohamed, N.E.A. El-Gamel. *Spectrochim. Acta*, **60A**, 3141 (2004); (d) G.G. Mohamed, N.E.A. El-Gamel. *Vib. Spectrosc*., **36**, 97 (2004); (e) M.A. Zayed, F.A. Nour El-Dien, G.G. Mohamed, N.E.A. El-Gamel. *J. Mol. Struct*., **841**, 41 (2007).
[24] N.E.A. El-Gamel, D. Gerlach. *J. Coord. Chem*., **61**, 2246 (2008).
[25] (a) B. Kojic-Prodic, Z. Ruzic-Toros. *Acta Crystallogr., Sect. B*, **38**, 2948 (1982); (b) I.L. Hwan Suh, K.-J. Kim, T.-S. Ko, B.-H. Kim. *Chung. Kwa. Yong (Kor.) (Chungnam J. Sci.)*, **16**, 30 (1989); (c) G. Reck, G. Dietz, G. Laban, W. Gunter, G. Bannier, E. Hohne. *Pharmazie*, **43**, 477 (1998); (d) J. Bordner, J.A. Richards, P. Weeks, E.B. Whipple. *Acta Crystallogr. Sect. C*, **40**, 989 (1984).

[26] (a) M.N. Caira, L.R. Nassimbeni, M. Timme. *J. Pharm. Sci.*, **84**, 884 (1995); (b) M.R. Caira, L.R. Nassimbeni, M. Timme. *J. Pharm. Sci.*, **84**, 884 (1995).
[27] (a) G.F. Fabiolo, V. Pattabhi, S.G. Manjunatha, G.V. Rao, K. Nagarajan. *Acta Crystallogr., Sect. C*, **54**, 2001 (1998); (b) P. Luger, K. Daneck, W. Engel, G. Trummlitz, K. Wagner. *Eur. J. Pharm. Sci.*, **4**, 175 (1996).
[28] G. Tamasi, F. Serinellu, M. Consumi, A. Magnani, M. Casolaro, R. Cini. *J. Inorg. Biochem.*, **102**, 1862 (2008).
[29] The Cambridge Crystallographic Data Centre CCDC, the Cambridge Structural Data base CSD, 12 Union Road, Cambridge, CB2 1EZ, UK. Release January 2006. http://www.ccdc.cam.ac.uk\products\csd\ (2006).
[30] R. Cini, F.P. Fanizzi, F.P. Intini, L. Maresca, G. Natile. *J. Am. Chem. Soc.*, **115**, 5123 (1993).
[31] J. Bordner, P.D. Hammen, E.B. Whipple. *J. Am. Chem. Soc.*, **111**, 6572 (1989).
[32] G.G. Mohamed. *Spectrochim. Acta*, **62A**, 1165 (2005).
[33] (a) M.R. Caira, M. Zanol, T. Peveri, A. Gazzaniga, F. Giordano. *J. Pharm. Sci.*, **87**, 1608 (1998); (b) F. Giordano, A. Gazzaniga, J.R. Moyano, P. Ventura, M. Zanol, T. Peveri, L. Carima. *J. Pharm. Sci.*, **87**, 333 (1998); (c) O.N. El-Gazayerly. *Drug Dev. Ind. Pharm.*, **26**, 925 (2000); (d) F. Vrecer, M. Vrbinc, A. Meden. *Int. J. Pharm.*, **256**, 3 (2003); (e) I. Kyrikou, S.K. Hadjikakou, D. Kovala-Demertzi, K. Viras, T. Mavromoustakos. *Chem. Phys. Lipids*, **132**, 157 (2004).
[34] L.J. Bellamy. *The Infrared Spectra of Complex Molecules*, Chapman and Hall, London (1975).
[35] (a) K. Nakamoto. *Infrared and Raman Spectra of Inorganic and Coordination Compounds*, 4th Edn, Wiley, New York (1980); (b) G. Maistrails, N. Katsaros, S.P. Perlepes, D. Kovala-Demertzi. *J. Inorg. Biochem.*, **45**, 1 (1992).
[36] P. Christofis, M. Katsarou, A. Papayriakou, Y. Sanakis, N. Katsaros, G. Psomas. *J. Inorg. Biochem.*, **99**, 2197 (2005).
[37] (a) P. Tauridou, U. Russo, G. Valle, D. Kovala-Demertzi. *J. Organomet. Chem.*, **460**, C16 (1993); (b) D. Kovala-Demertzi, P. Tauridou, J.M. Tsangari, A. Moukarika. *Main Group Met. Chem.*, **5**, 315 (1993); (c) P. Tauridou, U. Russo, D. Marton, G. Valle, D. Kovala-Demertzi. *Inorg. Chim. Acta*, **231**, 139 (1995); (d) D. Kovala-Demertzi, P. Tauridou, A. Moukarika, J.M. Tsangaris, C.P. Raptopoulou, A. Terzis. *J. Chem. Soc., Dalton Trans.*, 123 (1995); (e) D. Kovala-Demertzi, P. Tauridou, U. Russo, M. Gielen. *Inorg. Chim. Acta*, **239**, 177 (1995); (f) N. Kourkoumelis, A. Hatzidimitriou, D. Kovala-Demertzi. *J. Organomet. Chem.*, **514**, 163 (1996); (g) D. Kovala-Demertzi, N. Kourkoumelis, P. Tavridou, A. Moukarika, P.D. Akrivos, U. Ruesso. *Spectrochim. Acta*, **54A**, 1801 (1998).
[38] J.M. Geckle, D.M. Rescek, E.B. Whipple. *Magn. Reson. Chem.*, **27**, 150 (1989).
[39] (a) S.A. Abdelfattah, S.Z. El-Khateeb, S.A. Abdel Razeg, M.S. Stawakkol. *Spectrosc. Lett.*, **21**, 421 (1988); (b) P.J. Saindon, N.S. Cauchon, P.A. Sutton, C.-J. Chang, G.E. Peck, S.R. Byrn. *Pharm. Res.*, **10**, 197 (1993).
[40] E. Redenti, M. Zanol, P. Ventura, G. Fronza, A. Comotti, P. Taddel, A. Bertoluzza. *Biospectroscopy*, **5**, 243 (1999).
[41] (a) M.R. Pijak, P. Turcani, Z. Turcaniova, I. Buran, I. Gogolak, A. Mihal, F. Gazdik. *Bratislavske Lekarske Listy*, **103**, 469 (2002); (b) U. Semi. *Clin. Drug Invest.*, **19**, 51 (2000); (c) M. Martens. *Clin. Drug Invest.*, **19**, 47 (2000).
[42] B. Haraoui. *Clin. Drug Invest.*, **19**, 33 (2000).
[43] J.W.L. Nascimento, L.H. Santos, M.S. Northenberg, M.M. Coelho, S. Oga, C.A. Tagliati. *Pharmacology*, **68**, 64 (2003).
[44] S. Roy, R. Banerjee, M. Sarkar. *J. Inorg. Biochem.*, **100**, 1320 (2006).
[45] I. Lang, I. Papatsas. USXXCO US 2005187213 A1 20050825 (2005).
[46] I.E. Solovev, O.A. Solovev. *Naukove Torvarystvo Khirurhiv Ukrainy*, **9**, 10 (2004).